



Published in final edited form as:

Am J Surg Pathol. 2015 September ; 39(9): 1267–1274. doi:10.1097/PAS.0000000000000460.

Adamantinoma-like Ewing Family Tumors of the Head and Neck: A Pitfall in the Differential Diagnosis of Basaloid and Myoepithelial Carcinomas

Justin A. Bishop, M.D.^{1,*}, Rita Alaggio, M.D.², Lei Zhang, M.S.⁴, Raja R. Seethala, M.D.³, and
Cristina R. Antonescu, M.D.⁴

¹Department of Pathology, The Johns Hopkins University School of Medicine, Baltimore, MD

²Department of Pathology, Padova University Hospital, Padova, Italy

³Department of Pathology, University of Pittsburgh Medical Center, Pittsburgh, PA

⁴Department of Pathology, Memorial Sloan-Kettering Cancer Center, New York, NY, U.S.A

Abstract

The Ewing sarcoma family of tumors (EFTs) of the head and neck are rare and may be difficult to diagnose as they display significant histologic overlap with other more common undifferentiated small blue round cell malignancies. Occasionally, EFTs may exhibit overt epithelial differentiation in the form of diffuse cytokeratin immunoexpression or squamous pearls, resembling the so-called adamantinoma-like EFTs and being challenging to distinguish from *bona-fide* carcinomas.

Furthermore, the presence of *EWSR1* gene rearrangement correlated with strong keratin expression may suggest a myoepithelial carcinoma. Herein we analyze a series of 7 adamantinoma-like EFTs of the head and neck, most of them being initially misdiagnosed as carcinomas due to their anatomic location and strong cytokeratin immunoexpression, and subsequently reclassified as EFT by molecular techniques. The tumors arose in the sinonasal tract (n=2), parotid gland (n=2), thyroid gland (n=2), and orbit (n=1), in patients ranging from 7 to 56 years (mean, 31).

Microscopically they departed from the typical EFT morphology by growing as nests with peripheral nuclear palisading and prominent interlobular fibrosis, imparting a distinctly basaloid appearance. Moreover, two cases exhibited overt keratinization in the form of squamous pearls and one sinonasal tumor demonstrated areas of intraepithelial growth. All cases were positive for CD99, pan-cytokeratin, and p40. A subset of cases showed synaptophysin, S100 protein, and/or p16 reactivity, further confounding the diagnosis. FISH assays showed *EWSR1* and *FLII* rearrangements in all cases. Our results reinforce that a subset of head and neck EFT may show strong cytokeratin expression or focal keratinization, and thus indistinguishable from more common true epithelial neoplasms. Thus CD99 should be included in the immunopanel of a round cell malignancy regardless of strong cytokeratin expression or anatomic location, and a strong and diffuse CD99 positivity should prompt molecular testing for the presence of *EWSR1* gene rearrangements.

*Address correspondence to: Justin A. Bishop, M.D., The Johns Hopkins University School of Medicine, 401 N. Broadway, Weinberg 2249, Baltimore, MD 21231, Telephone (410) 955-8116, Facsimile (410) 955-0115, jbishop@jhmi.edu.

Keywords

Ewing sarcoma family tumor; adamantinoma-like Ewing sarcoma; primitive neuroectodermal tumor; EWSR1; FLI1; complex epithelial differentiation

INTRODUCTION

The Ewing sarcoma family of tumors (EFT) is a group of neoplasms defined by recurrent *EWSR1-ETS* related fusions, a genetic hallmark that has unified different clinical presentations and phenotypes among this spectrum, including intraosseous and extraosseous Ewing sarcomas and peripheral neuroectodermal tumors (PNET).(1) EFTs often occur in children and young adults and affect with predilection the long bones or pelvis.(1, 2) Approximately 5% of EFTs involve the head and neck where its histologic appearance overlaps with other small blue round cell tumors commonly occurring at this site, such as alveolar rhabdomyosarcoma, olfactory neuroblastoma, NUT midline carcinoma, lymphoma, melanoma, and many others.(3–7) Despite the overlapping morphologies of these undifferentiated round cell malignancies, precise tumor classification is crucial for establishing prognosis and in guiding appropriate therapeutic strategies. Indeed, EFT is typically treated with specific chemotherapy protocols that may differ from the therapeutic regimens of other head and neck malignancies.(8, 9)

In most cases the diagnosis of EFTs is suggested by its typical monotonous histologic appearance, with sheets and lobules of uniform round cells exhibiting vesicular nuclei and scant clear cytoplasm, and diffuse and strong membranous immunoreactivity for CD99. However, a less recognized feature of EFT is its propensity to exhibit cytokeratin immunoreactivity in up to 20–30% of cases.(10–12) While this immunoreactivity is usually focal and mainly with low molecular weight cytokeratins, a rare group of EFT known as “adamantinoma-like” EFTs, show complex epithelial differentiation, exhibiting histologic (i.e., squamous pearls, intracellular bridges) and/or immunophenotypic (i.e., diffuse p40 and/or high molecular weight cytokeratin) evidence of squamous differentiation.(10, 13–18) Until recently, adamantinoma-like EFTs had only been encountered in the long bones or surrounding soft tissues. There have now been three separate case reports of adamantinoma-like EFTs in the head and neck: two in the neck soft tissues and one in the parotid gland. (16–18) In addition, there are two case reports of a tumor described as “carcinoma of the thyroid with Ewing family tumor elements” that likely represents the same entity.(19–21) We present the first case series of adamantinoma-like EFT in the head and neck, including five previously unpublished cases.

METHODS

Cases

We identified seven cases of adamantinoma-like EFT arising in the head and neck (see Table 1). Case 1 was identified within a tissue microarray containing 151 consecutive cases of sinonasal carcinomas from Johns Hopkins Hospital, constructed as previously described. (22) The remaining six cases were diagnosed prospectively in the authors’ respective

consultation practices (JAB, RSS, and CRA). One of these cases (case 4) was previously published as a case report,(18) and another case (case 3) was included as part of a series of soft tissue myoepithelial carcinomas due to its *EWSR1* gene rearrangement.(23, 24) Each case was examined by routine light microscopy, immunohistochemistry, and fluorescence in situ hybridization (FISH).

Immunohistochemistry

Immunohistochemistry for CD99 (clone 12E7; Leica, Buffalo Grove, IL; prediluted), pancytokeratin (PCK26; Ventana, Tuscon, AZ; prediluted); p40 (Ab-1; Oncogene Research Products, Cambridge, MA; 1:2000 dilution), synaptophysin (clone 27G12; Leica Microsystems; prediluted); chromogranin (clone LK2H10; Ventana; prediluted); S100 protein (clone 4C4.9; Ventana; prediluted), muscle specific actin (clone HHF35; Ventana, prediluted); desmin (clone D33, Dako, Carpinteria, CA; 1:100 dilution), NUT-1 (clone C52B1, Cell Signaling Technologies, Inc., Danvers, MA, 1:50 dilution), and p16 (clone INK4a; MTM Laboratories, Heidelberg, Germany); was performed on five-micron sections utilizing standard protocols on a Ventana Benchmark XT autostainer. In addition, in situ hybridization for high-risk types of human papillomavirus was also performed utilizing the Ventana HR HPV III probe set that captures HPV genotypes 16, 18, 31, 33, 35, 39, 45, 51, 52, 56, 58 and 66. The sinonasal tissue microarray was also stained with CD99.

Fluorescence in situ hybridization

For all 7 cases, the diagnosis was confirmed by fluorescence in situ hybridization (FISH) assays for both *EWSR1* and *FLII* (Figure 1). The FISH assays were performed on each consult case prospectively, as well as the cases from the tissue microarray that were positive for CD99 by immunohistochemistry. FISH was performed by applying custom probes using bacterial artificial chromosomes (BACs), covering and flanking the *EWSR1* and *FLII* gene. BAC clones were chosen according to UCSC genome browser (<http://genome.ucsc.edu>), see Table 1. The BAC clones were obtained from BACPAC sources of Children's Hospital of Oakland Research Institute (CHORI) (Oakland, CA)(<http://bacpac.chori.org>). DNA from individual BACs was isolated according to the manufacturer's instructions, labeled with different fluorochromes in a nick translation reaction, denatured, and hybridized to pretreated slides. Slides were then incubated, washed, and mounted with DAPI in an antifade solution, as previously described.(24) The genomic location of each BAC set was verified by hybridizing them to normal metaphase chromosomes. Two hundred successive nuclei were examined using a Zeiss fluorescence microscope (Zeiss Axioplan, Oberkochen, Germany), controlled by Isis 5 software (Metasystems, Newton, MA). A positive score was interpreted when at least 20% of the nuclei showed a break-apart signal. Nuclei with incomplete set of signals were omitted from the score.

RESULTS

Only three of 151 (2%) cases from the sinonasal carcinoma tissue microarray were positive for CD99. One of these CD99-positive cases (case 1) was confirmed by positive *EWSR1* and *FLII* FISH assays to be an adamantinoma-like EFT, while the other two lacked *EWSR1*

gene abnormalities. This adamantinoma-like EFT was originally diagnosed as a poorly differentiated squamous cell carcinoma.

The clinical characteristics of the adamantinoma-like EFTs are summarized in Table 2. The EFTs arose in the sinonasal tract (n=2), parotid gland (n=2), thyroid gland (n=2), and orbit (n=1) of patients ranging from 7 to 56 years (mean, 31). The tumors arose in 5 females and 2 males. The initial presentations were non-specific: the parotid tumors presented as painless masses; the orbital tumor and one sinonasal tumor presented with proptosis; the other sinonasal tumor presented as epistaxis and nasal obstruction; and the thyroid tumors presented as growing neck masses. Six of 7 had their tumors surgically resected. Chemotherapy and radiation therapy were given in 4 cases; for the remaining patients (Cases 5, 6, and 7), the diagnoses were very recent and adjuvant therapy has not yet commenced. Follow-up information was available for 4 patients. Two patients have no evidence of disease, one patient is alive but with residual tumor, and one patient died of her disease 52 months following initial diagnosis.

Histologically the adamantinoma-like EFTs resembled typical EFTs in certain ways. They consisted of proliferations of uniform, small cells with a minimal to moderate amount of pale eosinophilic to clear cytoplasm (Figures 2A–B). The nuclei were round to oval with finely dispersed chromatin and a single, generally indistinct nucleolus (Figures 2B–D). Vague streaming was observed in 3 cases, and focal rosette formation was also observed in 3 cases (Figure 2C). The mitotic rates ranged from 5–12 mitoses per 10 high power fields (mean, 6), and tumor necrosis was noted in 4 tumors. Perineural invasion was seen in 2 cases each and bone involvement was observed only in the two sinonasal tumors. In other respects, however, the histology of the tumors departed dramatically from usual EFTs. First, while the architecture was variable and included sheets and trabeculae, all cases exhibited distinctive areas of nested growth with prominent fibrosis separating tumor lobules (Figures 2A–B), as well as areas of peripheral palisading of tumor nuclei in some of the tumor nests that imparted a basaloid appearance to the neoplasms (Figure 2C). Two cases demonstrated hyaline basement membrane-like material interspersed among the tumor cells (Figure 2D). Rare foci of overt keratinization in the form of squamous pearls were present in two cases (Figures 3A–B). Unexpectedly, one of the sinonasal tumors exhibited areas of intraepithelial growth in the overlying sinonasal epithelium (Figure 3B). One of the thyroid tumors (case 6) was unusual exhibiting in addition to the basaloid areas, large zones of microcystic growth set in a prominent myxoid stroma (Figures 3C–D). In both thyroid cases (cases 6 and 7) the tumor cells showed a peculiar colonization of the underlying follicles.

The immunohistochemical findings are summarized in Table 3. Each case was diffusely positive for pan-cytokeratin and CD99 (Figures 4A–B). Of the 6 cases tested for p40, each was positive, with diffuse staining seen in 5 of 6 (Figures 4C). Synaptophysin immunostaining was seen in 3 of 6 cases tested (Figure 4D), and was focal in 2. Focal chromogranin immunostaining was present in only 1 of 6 tested cases. Three of 7 tumors were S100-positive, with focal expression in two of those cases. Actin was focally positive in one case, but desmin was negative in all tumors. NUT-1 immunostaining was negative in all 5 cases tested, and although diffuse p16 immunostaining was present in 2 of 5 cases tested, all 5 were negative for high risk HPV by in situ hybridization.

DISCUSSION

The Ewing sarcoma family of tumors has been well recognized for several decades, but only recently has its histologic and immunophenotypic spectrum been fully appreciated. Recent studies have demonstrated rare examples exhibiting prominent squamous epithelial differentiation, for which the designation of “adamantinoma-like” EFT or EFT with complex epithelial differentiation has been proposed.(10, 13–18) The degree to which these tumors truly resemble adamantinomas is certainly debatable, but this terminology is historical: the term adamantinoma-like EFT was used since the first few reported cases with this phenotype occurred in the long tubular bones, including tibia and simulated the diagnosis of extragnatic adamantinoma.(10, 13, 14) Only recently similar cases were documented in the head and neck.(16–20) This study is the largest series (n=7) of adamantinoma-like EFT to date and focuses specifically on head and neck due to its challenging differential diagnoses encountered in these locations. Similar to classic EFT, head and neck adamantinoma-like EFT appears to generally affect young patients and may arise in a wide range of anatomic subsites including periorbital soft tissues, thyroid gland, parotid gland, and even mucosal sites like the sinonasal tract.

When dealing with a poorly differentiated head and neck tumor with a basaloid growth or small round cell appearance, arriving at the correct diagnosis typically relies on demonstrating some evidence of lineage-specific differentiation. Sometimes lines of differentiation can be detected on routine histology, by demonstrating evidence of surface epithelial origin (e.g., carcinoma-in-situ), squamous eddies or intracellular bridges, ducts or glands, or neuroendocrine features like nuclear molding or salt-and-pepper chromatin. Often, however, immunohistochemical studies are needed to determine the nature of a poorly differentiated basaloid or small blue round cell tumor. Unfortunately when it comes to adamantinoma-like EFT, this time-honored strategy is likely to obfuscate rather than clarify. Indeed, the histologic features (basaloid nests, squamous pearls, intraepithelial growth) and immunoprofile (diffuse cytokeratin and p40) of adamantinoma-like EFT strongly point to a carcinoma, especially squamous cell carcinoma, a far more common malignancy of the head and neck. Even a potentially helpful feature like pseudorosette formation can be easily misinterpreted as the pseudoglandular spaces of basaloid squamous cell carcinoma. Perhaps the single most important key to avoiding this pitfall is recognition of the characteristic nuclear monotony of adamantinoma-like EFT. High-grade squamous cell carcinomas usually exhibit variability in nuclear size and shape reflecting the complex genetic changes typically harbored by these tumors. Adamantinoma-like EFT, on the other hand, exhibits strikingly isomorphic nuclei, similar to other translocation-associated sarcomas.(25) In addition, when present, expression of synaptophysin in the setting of absent or focal chromogranin and diffuse p40 immunostaining is an unusual staining pattern that should raise suspicion for an uncommon tumor like adamantinoma-like EFT. Once the diagnosis of an adamantinoma-like EFT is considered, CD99 immunostaining is very helpful for supporting that diagnostic possibility. All 7 cases of adamantinoma-like EFT demonstrated diffuse membranous CD99 immunostaining, while this pattern is relatively uncommon in other head and neck carcinomas. Indeed, only 2 of 150 (1%) sinonasal carcinomas from the tissue microarray were CD99-positive. Finally, while those features are

suggestive of an adamantinoma-like EFT, molecular studies demonstrating rearrangements involving *EWSR1* and *FLII* are required to make a definitive diagnosis.

Other considerations in the differential diagnosis of adamantinoma-like EFT include NUT midline carcinoma and myoepithelial carcinoma. Like adamantinoma-like EFT, NUT midline carcinoma may affect many subsites of the head and neck and is also characterized by nuclear monotony with squamous differentiation sometimes manifesting as focal keratinization.(22, 26, 27) Moreover, CD99 expression may rarely be seen in NUT midline carcinoma.(28, 29) Fortunately, the commercially available NUT-1 immunostain is highly sensitive and specific for NUT midline carcinoma.(22, 30) Indeed, all adamantinoma-like EFTs tested were negative for NUT-1. A round cell/undifferentiated form of myoepithelial carcinoma of either salivary gland or soft tissue may also be difficult to distinguish from adamantinoma-like EFT. Both tumors may exhibit nuclear uniformity, clear cytoplasm, eosinophilic matrix-like material or myxoid stroma, and immunostaining for the myoepithelial markers S100 protein, p40, and actin. The similarities extend at the molecular level, because soft tissue myoepithelial tumors often harbor rearrangements of *EWSR1*.(24, 31, 32) As a result, for a definitive diagnosis of adamantinoma-like EFT, demonstration of *EWSR1* rearrangement by itself is not sufficient. The fusion partner gene – usually *FLII* for adamantinoma-like EFT and *POU5F1*, *PBX1*, *PBX3* or *ZNF444* for myoepithelial carcinoma – must be determined for a more definitive classification.(24, 31, 32)

In the sinonasal tract, parotid gland, and thyroid gland, other site-specific diagnoses must be distinguished from adamantinoma-like EFT. In the sinonasal tract, sinonasal undifferentiated carcinoma is a diagnostic consideration; like adamantinoma-like EFT, it is a poorly differentiated carcinoma that may exhibit focal squamous or even neuroendocrine differentiation. On the other hand, sinonasal undifferentiated carcinoma usually exhibits more nuclear pleomorphism than is seen in EFT, and it is usually negative or at most focal for CD99 and p40. In the superior nasal cavity, lower grade forms of olfactory neuroblastoma exhibit features that overlap with conventional EFTs like pseudorosettes, monotonous tumor nuclei, and neuroendocrine differentiation. On the other hand, olfactory neuroblastoma is less likely to be confused with the adamantinoma-like form of EFT because it does not express cytokeratin or p40 diffusely, frequently contains S100-positive sustentacular cells, is often diffusely chromogranin positive. In the parotid gland, basal cell adenocarcinoma and a solid form of adenoid cystic carcinoma may be considered. Basal cell adenocarcinomas are typically low-grade, without the elevated mitotic rates, necrosis, and high degree of infiltration, as seen in the two parotid adamantinoma-like EFTs. While solid forms of adenoid cystic carcinoma may be high-grade, they generally exhibit at least focal cribriform growth. In addition, both salivary gland tumors are biphasic with a patchy p40 immunostaining pattern and true ducts that may be highlighted by EMA or CD117. In the thyroid gland, the differential diagnosis includes medullary carcinoma, poorly differentiated thyroid carcinoma, and tumors with thymic differentiation (i.e., thymic neoplasm extending into the thyroid, carcinoma showing thymic-like differentiation, or spindle epithelial tumor with thymus-like differentiation). An absence TTF-1, CEA, and calcitonin immunostaining excludes medullary carcinoma, while diffuse CD99 and p40 immunostaining with a lack of TTF-1, thyroglobulin, and PAX-8 immunostaining rules out a poorly differentiated

carcinoma of thyroid follicular origin. The absence of CD5 immunoreactivity in the face of CD99 expression is inconsistent with carcinoma showing thymic-like differentiation or thymic carcinoma, but distinguishing adamantinoma-like EFT from spindle epithelial tumor with thymus-like differentiation may be more difficult because both tumors may show squamous differentiation and often express high-molecular weight cytokeratins as well as CD99.(33–35) In this differential diagnosis, morphologic features are most helpful because while spindle epithelial tumor with thymus-like differentiation may have epithelioid areas, it is predominantly spindled and frequently demonstrates true glandular differentiation.(34, 35) Moreover, unlike adamantinoma-like EFT, spindle epithelial tumors with thymus-like differentiation do not exhibit necrosis and have very low mitotic rates.(34, 35) Of course, the diagnostic molecular signature of EFT excludes all the other tumors described above.

The differential diagnosis of adamantinoma-like EFT is not limited to epithelial neoplasms. Desmoplastic small round cell tumor, for example, rarely affects the head and neck (36–38) and exhibits prominent fibrosis and express positivity for cytokeratins, CD99, and occasionally synaptophysin. Unlike adamantinoma-like EFT, however, desmoplastic small round cell tumor is typically positive for desmin and WT-1. While desmoplastic small round cell tumor also harbors translocations involving the *EWSR1* gene, the fusion partner is *WT1*. Synovial sarcoma is another sarcoma that also by definition exhibits epithelial differentiation by light microscopy and immunohistochemistry. In addition, synovial sarcoma is frequently CD99 positive.(39, 40) Typical examples of synovial sarcoma are unlikely to be confused with adamantinoma-like EFT as they are predominantly spindled and fascicular, with or without evidence of glandular differentiation. However, poorly differentiated synovial sarcomas may be impossible to distinguish from adamantinoma-like EFT based on histology and immunohistochemistry alone. In that circumstance, molecular diagnostics are once again critical, because synovial sarcoma is characterized by translocations involving the *SYT* gene.

In summary, adamantinoma-like EFT may occur in the head and neck, where its correct classification remains very challenging. To ensure that patients with EFT receive the proper chemotherapy protocols, one must be aware that overt epithelial differentiation in a head and neck tumor does not by itself exclude an EFT. For any poorly differentiated or undifferentiated head and neck tumor, nuclear monotony and CD99 immunoreactivity should prompt consideration for molecular studies that include analysis of both *EWSR1* and *FLII*, even in the presence of strong cytokeratin expression or focal keratinization.

Acknowledgments

We thank Dr. Olga Blatnik, M.D. (Staff Pathologist in the Institute of Oncology, Ljubljana, Slovenia) for contributing one of the cases.

References

1. Ushigome, S.; Machinami, R.; Sorensen, PH. Ewing sarcoma/primitive neuroectodermal tumor (PNET). In: Fletcher, CD.; Unni, KK.; Mertens, F., editors. World Health Organization classification of tumours Pathology and genetics of bone and soft tissue tumours. Lyon, France: IARC Press; 2002. p. 298-300.

2. Cotterill SJ, Ahrens S, Paulussen M, et al. Prognostic factors in Ewing's tumor of bone: analysis of 975 patients from the European Intergroup Cooperative Ewing's Sarcoma Study Group. *J Clin Oncol.* 2000; 18:3108–3114. [PubMed: 10963639]
3. Hafezi S, Seethala RR, Stelow EB, et al. Ewing's family of tumors of the sinonasal tract and maxillary bone. *Head Neck Pathol.* 2011; 5:8–16. [PubMed: 21107767]
4. Vaccani JP, Forte V, de Jong AL, et al. Ewing's sarcoma of the head and neck in children. *Int J Pediatr Otorhinolaryngol.* 1999; 48:209–216. [PubMed: 10402117]
5. Iezzoni JC, Mills SE. "Undifferentiated" small round cell tumors of the sinonasal tract: differential diagnosis update. *Am J Clin Pathol.* 2005; 124 (Suppl):S110–121. [PubMed: 16468421]
6. Bridge JA, Bowen JM, Smith RB. The small round blue cell tumors of the sinonasal area. *Head Neck Pathol.* 2010; 4:84–93. [PubMed: 20237994]
7. Tilson MP, Bishop JA. Utility of p40 in the Differential Diagnosis of Small Round Blue Cell Tumors of the Sinonasal Tract. *Head Neck Pathol.* 2013
8. Rodriguez-Galindo C, Spunt SL, Pappo AS. Treatment of Ewing sarcoma family of tumors: current status and outlook for the future. *Med Pediatr Oncol.* 2003; 40:276–287. [PubMed: 12652615]
9. Huang M, Lucas K. Current therapeutic approaches in metastatic and recurrent ewing sarcoma. *Sarcoma.* 2011; 2011:863210. [PubMed: 21151650]
10. Folpe AL, Goldblum JR, Rubin BP, et al. Morphologic and immunophenotypic diversity in Ewing family tumors: a study of 66 genetically confirmed cases. *Am J Surg Pathol.* 2005; 29:1025–1033. [PubMed: 16006796]
11. Gu M, Antonescu CR, Guiter G, et al. Cytokeratin immunoreactivity in Ewing's sarcoma: prevalence in 50 cases confirmed by molecular diagnostic studies. *Am J Surg Pathol.* 2000; 24:410–416. [PubMed: 10716155]
12. Collini P, Sampietro G, Bertulli R, et al. Cytokeratin immunoreactivity in 41 cases of ES/PNET confirmed by molecular diagnostic studies. *Am J Surg Pathol.* 2001; 25:273–274. [PubMed: 11176079]
13. Bridge JA, Fidler ME, Neff JR, et al. Adamantinoma-like Ewing's sarcoma: genomic confirmation, phenotypic drift. *Am J Surg Pathol.* 1999; 23:159–165. [PubMed: 9989842]
14. Hauben E, van den Broek LC, Van Marck E, et al. Adamantinoma-like Ewing's sarcoma and Ewing's-like adamantinoma. The t(11; 22), t(21; 22) status. *J Pathol.* 2001; 195:218–221. [PubMed: 11592101]
15. Fujii H, Honoki K, Enomoto Y, et al. Adamantinoma-like Ewing's sarcoma with EWS-FLI1 fusion gene: a case report. *Virchows Arch.* 2006; 449:579–584. [PubMed: 17016721]
16. Weinreb I, Goldstein D, Perez-Ordóñez B. Primary extraskelletal Ewing family tumor with complex epithelial differentiation: a unique case arising in the lateral neck presenting with Horner syndrome. *Am J Surg Pathol.* 2008; 32:1742–1748. [PubMed: 18769338]
17. Kikuchi Y, Kishimoto T, Ota S, et al. Adamantinoma-like Ewing family tumor of soft tissue associated with the vagus nerve: a case report and review of the literature. *Am J Surg Pathol.* 2013; 37:772–779. [PubMed: 23552387]
18. Lezcano C, Clarke MR, Zhang L, et al. Adamantinoma-Like Ewing Sarcoma Mimicking Basal Cell Adenocarcinoma of the Parotid Gland: A Case Report and Review of the Literature. *Head Neck Pathol.* 2014
19. Eloy C, Cameselle-Teijeiro J, Vieira J, et al. Carcinoma of the thyroid with Ewing/PNET family tumor elements: a tumor of unknown histogenesis. *Int J Surg Pathol.* 2014; 22:579–581. [PubMed: 23637257]
20. Eloy C, Oliveira M, Vieira J, et al. Carcinoma of the thyroid with ewing family tumor elements and favorable prognosis: report of a second case. *Int J Surg Pathol.* 2014; 22:260–265. [PubMed: 23637256]
21. Cruz J, Eloy C, Aragües JM, et al. Small-cell (basaloid) thyroid carcinoma: a neoplasm with a solid cell nest histogenesis? *Int J Surg Pathol.* 2011; 19:620–626. [PubMed: 21531696]
22. Bishop JA, Westra WH. NUT midline carcinomas of the sinonasal tract. *Am J Surg Pathol.* 2012; 36:1216–1221. [PubMed: 22534723]
23. Bisogno G, Tagarelli A, Schiavetti A, et al. Myoepithelial carcinoma treatment in children: a report from the TREP project. *Pediatr Blood Cancer.* 2014; 61:643–646. [PubMed: 24136896]

24. Antonescu CR, Zhang L, Chang NE, et al. EWSR1-POU5F1 fusion in soft tissue myoepithelial tumors. A molecular analysis of sixty-six cases, including soft tissue, bone, and visceral lesions, showing common involvement of the EWSR1 gene. *Genes, chromosomes & cancer*. 2010; 49:1114–1124. [PubMed: 20815032]
25. Antonescu CR, Dal Cin P. Promiscuous genes involved in recurrent chromosomal translocations in soft tissue tumours. *Pathology*. 2014; 46:105–112. [PubMed: 24378390]
26. French CA, Kutok JL, Faquin WC, et al. Midline carcinoma of children and young adults with NUT rearrangement. *Journal of clinical oncology : official journal of the American Society of Clinical Oncology*. 2004; 22:4135–4139. [PubMed: 15483023]
27. Stelow EB, Bellizzi AM, Taneja K, et al. NUT rearrangement in undifferentiated carcinomas of the upper aerodigestive tract. *Am J Surg Pathol*. 2008; 32:828–834. [PubMed: 18391746]
28. Teo M, Crotty P, O’Sullivan M, et al. NUT midline carcinoma in a young woman. *J Clin Oncol*. 2011; 29:e336–339. [PubMed: 21263084]
29. Solomon LW, Magliocca KR, Cohen C, et al. Retrospective analysis of nuclear protein in testis (NUT) midline carcinoma in the upper aerodigestive tract and mediastinum. *Oral Surg Oral Med Oral Pathol Oral Radiol*. 2014
30. Haack H, Johnson LA, Fry CJ, et al. Diagnosis of NUT midline carcinoma using a NUT-specific monoclonal antibody. *Am J Surg Pathol*. 2009; 33:984–991. [PubMed: 19363441]
31. Brandal P, Panagopoulos I, Bjerkehagen B, et al. t(19;22)(q13;q12) Translocation leading to the novel fusion gene EWSR1-ZNF444 in soft tissue myoepithelial carcinoma. *Genes, chromosomes & cancer*. 2009; 48:1051–1056. [PubMed: 19760602]
32. Agaram NP, Chen HW, Zhang L, et al. EWSR1-PBX3: A novel gene fusion in myoepithelial tumors. *Genes Chromosomes Cancer*. 2014
33. Dorfman DM, Shahsafaei A, Chan JK. Thymic carcinomas, but not thymomas and carcinomas of other sites, show CD5 immunoreactivity. *Am J Surg Pathol*. 1997; 21:936–940. [PubMed: 9255257]
34. Folpe AL, Lloyd RV, Bacchi CE, et al. Spindle epithelial tumor with thymus-like differentiation: a morphologic, immunohistochemical, and molecular genetic study of 11 cases. *Am J Surg Pathol*. 2009; 33:1179–1186. [PubMed: 19417583]
35. Cheuk W, Jacobson AA, Chan JK. Spindle epithelial tumor with thymus-like differentiation (SETTLE): a distinctive malignant thyroid neoplasm with significant metastatic potential. *Mod Pathol*. 2000; 13:1150–1155. [PubMed: 11048811]
36. Wolf AN, Ladanyi M, Paull G, et al. The expanding clinical spectrum of desmoplastic small round-cell tumor: a report of two cases with molecular confirmation. *Hum Pathol*. 1999; 30:430–435. [PubMed: 10208465]
37. Pang B, Leong CC, Salto-Tellez M, et al. Desmoplastic small round cell tumor of major salivary glands: report of 1 case and a review of the literature. *Appl Immunohistochem Mol Morphol*. 2011; 19:70–75. [PubMed: 20861791]
38. Mihok NA, Cha I. Desmoplastic small round cell tumor presenting as a neck mass: a case report. *Diagn Cytopathol*. 2001; 25:68–72. [PubMed: 11466817]
39. Folpe AL, Schmidt RA, Chapman D, et al. Poorly differentiated synovial sarcoma: immunohistochemical distinction from primitive neuroectodermal tumors and high-grade malignant peripheral nerve sheath tumors. *Am J Surg Pathol*. 1998; 22:673–682. [PubMed: 9630174]
40. Olsen SH, Thomas DG, Lucas DR. Cluster analysis of immunohistochemical profiles in synovial sarcoma, malignant peripheral nerve sheath tumor, and Ewing sarcoma. *Mod Pathol*. 2006; 19:659–668. [PubMed: 16528378]

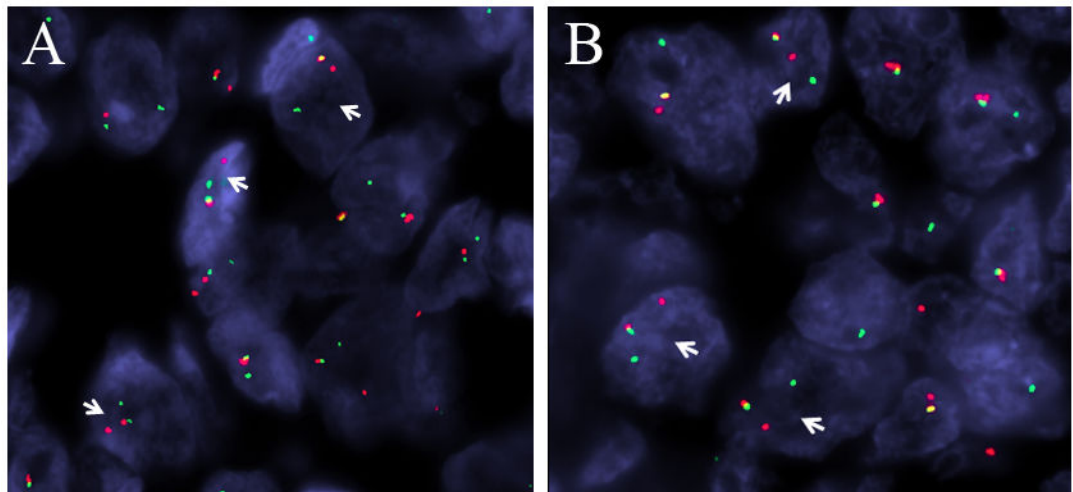


Figure 1. Each adamantinoma-like Ewing family tumor was positive for rearrangements of both *EWSR1* (A) and *FLI1* (B), as indicated by the separated red (centromeric) and green (telomeric) signals (arrows) seen on break-apart fluorescent in situ hybridization studies.

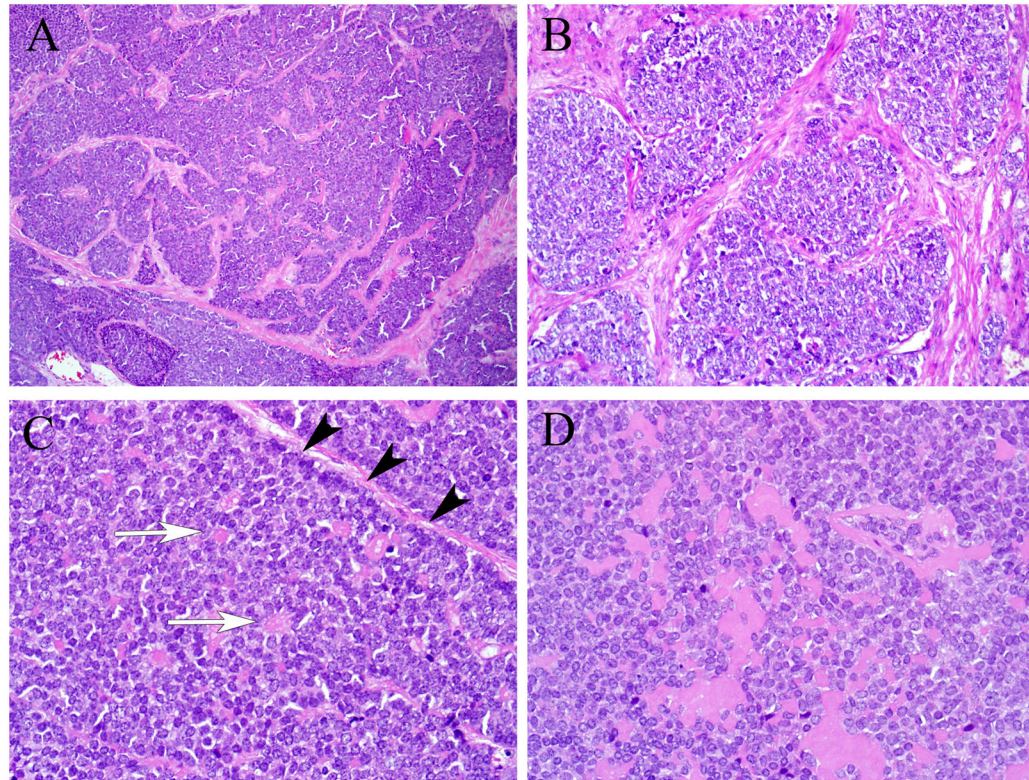


Figure 2.

All of the adamantinoma-like Ewing family tumors demonstrated areas of nested tumor growth with prominent fibrosis separating the nests (A and B). All of the tumors showed some areas of peripheral nuclear palisading (black arrowheads), and three of them had vague rosette formation (white arrows) (C). Two of the adamantinoma-like Ewing family tumors appeared to produce hyaline matrix-like material (D).

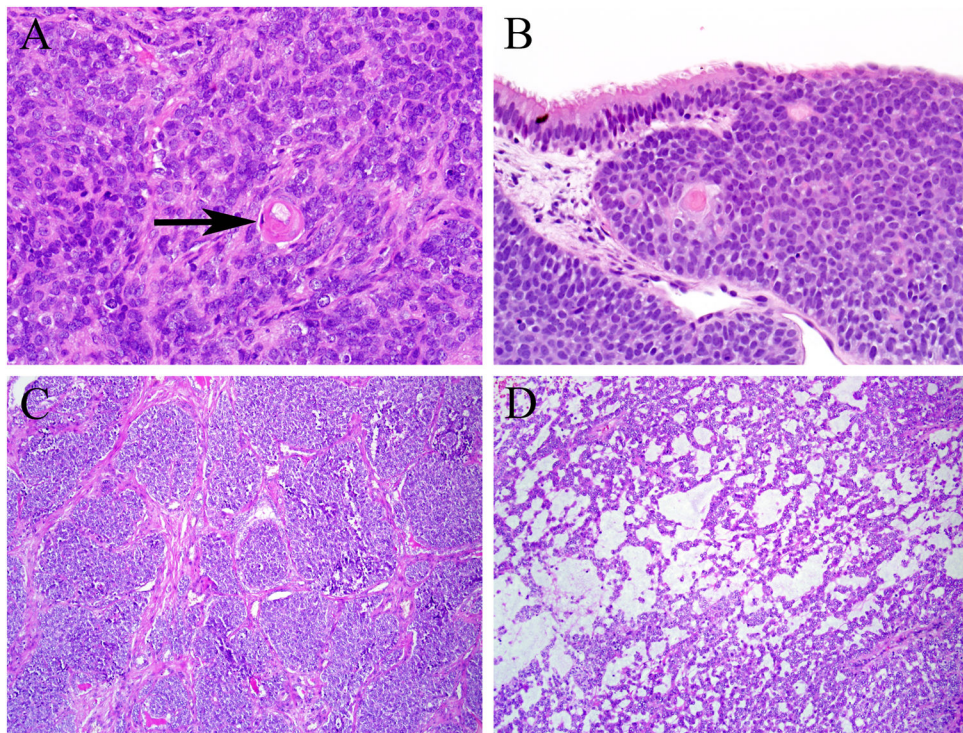


Figure 3.

Two of the adamantinoma-like Ewing family tumors exhibited overt squamous differentiation with squamous pearls (arrow) (A), and one of those tumors also demonstrated areas of intraepithelial tumor growth (B). The adamantinoma-like Ewing family tumor that arose in the thyroid gland had a minor component of nested, basaloid architecture (C), but also had a prominent component of peculiar microcystic growth with myxoid stroma (D).

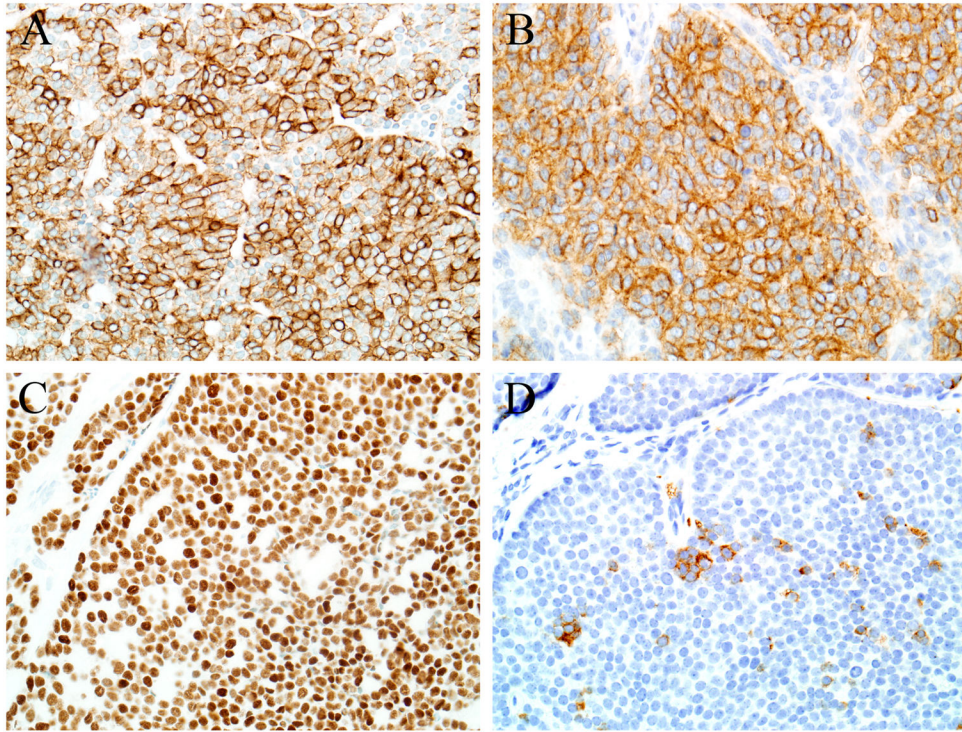


Figure 4. Each adamantinoma-like Ewing family tumor was diffusely positive for pan cytokeratin (A) and CD99 (B). All tumors tested for p40 were positive, and 4 of 5 were diffusely p40-positive (C). Two of the tumors showed some evidence of neuroendocrine differentiation in the form of synaptophysin immunoreactivity, but it was focal in both cases (D).

Table 1

Custom bacterial artificial chromosome probes used for fluorescence in situ hybridization analysis

| BAC clones | Cytoband | Genes | GP-starting | GP-ending |
|-------------|----------|---------|-------------|-----------|
| RP11-945M21 | 22q12.1 | C-EWSR1 | 29419092 | 29630216 |
| RP11-965D15 | 22q12.1 | C-EWSR1 | 29191411 | 29383544 |
| RP11-77M13 | 22q12.1 | C-EWSR1 | 28987722 | 29143837 |
| RP11-155B12 | 22q12.2 | T-EWSR1 | 29899043 | 30057948 |
| RP11-551L12 | 22q12.2 | T-EWSR1 | 30038549 | 30179920 |
| RP11-794O14 | 22q12.2 | T-EWSR1 | 30190755 | 30400388 |
| RP11-73P14 | 11q24.3 | T-FLI1 | 128730337 | 128903274 |
| RP11-115H10 | 11q24.3 | T-FLI1 | 128991621 | 129165376 |
| RP11-671N22 | 11q24.3 | T-FLI1 | 129161297 | 129316540 |
| RP11-264E20 | 11q24.3 | C-FLI1 | 128425388 | 128585568 |
| RP11-1007G5 | 11q24.3 | C-FLI1 | 128261657 | 128446272 |
| RP11-876L16 | 11q24.3 | C-FLI1 | 127986651 | 128178691 |

Abbreviations: BAC, bacterial artificial chromosome; GP, genomic position; T, telomeric; C, centromeric.

Table 2
Clinical characteristics of the head and neck adamantinoma-like Ewing family tumors.

| Case # | Site | Age | Sex | Initial presentation | Treatment | Clinical course | Outcome | Follow-up (months) |
|--------|-----------------------------|-----|----------------|------------------------|--|--|------------------|--------------------|
| 1 | Nasal cavity, ethmoid sinus | 37 | F ⁶ | Obstruction, epistaxis | Initially surgery only. Recurrences: surgery + XRT + chemo (docetaxel, carboplatin, capecitabine, methotrexate); | Local recurrence at 24 months; dural metastases at 46 months | DWD ⁶ | 52 |
| 2 | Ethmoid sinus, orbit, brain | 21 | M ¹ | Proptosis | XRT ² + chemo ³ (VDC/IE ⁴) | Stable local disease, no evidence of metastases | AWD ⁵ | 12 |
| 3 | Orbit | 7 | F | Proptosis | Surgery + XRT + chemo (ifosfamide + cyclophosphamide + etoposide, then ifosfamide + vincristine + etoposide) | No residual disease | NED ⁷ | 61 |
| 4 | Parotid gland | 56 | F | Painless neck mass | Surgery + XRT + chemo (VDC/IE) | No residual disease | NED | 1 |
| 5 | Parotid gland | 40 | F | Painless facial mass | Surgery. Additional therapy pending | Forthcoming | NED | 0 |
| 6 | Thyroid gland | 19 | M | Neck mass | Surgery. Additional therapy pending | Forthcoming | NED | 0 |
| 7 | Thyroid gland | 36 | F | Goiter | Surgery. Additional therapy pending | Forthcoming | unknown | 0 |

¹ M = male;

² XRT=radiation therapy;

³ chemo=systemic chemotherapy;

⁴ VDC/IE = alternating vincristine + doxorubicin + cyclophosphamide and ifosfamide + etoposide;

⁵ AWD = alive with disease;

⁶ F=female;

⁷ NED= no evidence of disease.

Histologic and immunohistochemical characteristics of the head and neck adamantinoma-like Ewing family tumors.

Table 3

| Case # | CD99 | Pan-CK ¹ | p40 | SYN ² | CHR ³ | S100 | Actin | Desmin | NUT-1 |
|--------|------|---------------------|-----|------------------|------------------|------|-------|--------|-------|
| 1 | + | + | + | - | - | + | - | - | - |
| 2 | + | + | + | - | - | - | - | - | - |
| 3 | + | + | ND | ND | ND | F+ | - | - | ND |
| 4 | + | + | + | F+ | - | - | - | - | - |
| 5 | + | + | + | F+ | - | - | - | - | - |
| 6 | + | + | F+ | - | - | F+ | F+ | - | - |
| 7 | + | + | + | + | F+ | - | - | -- | ND |

¹ CK=cytokeratin;

² SYN=synaptophysin;

³ CHR=chromogranin;

⁴ F+= focally positive (i.e., <5% of cells)